Lateral entrainment rate in shallow cumuli: Dependence on dry air sources and probability density functions

Chunsong Lu,[1,2] Yangang Liu,[2] Shengjie Niu,[1] and Andrew M. Vogelmann[2]

Received 22 August 2012; revised 27 September 2012; accepted 28 September 2012; published 30 October 2012.

[1] Entrainment processes in convective clouds often occur stochastically and entrainment rate estimates depend on the distance from the cloud from which the dry air is entrained. However, no observational studies exist on either the distance dependence or probability density function of entrainment rate, hindering understanding and the parameterization of convection. Here entrainment rate in cloud cores is estimated using a recently developed mixing fraction approach that is applied to in situ aircraft measurements of cumuli from the RACORO field program. The results are used to examine, for the first time, probability density functions of entrainment rate and their dependence on the distance from the edge of the cloud core from which the dry air is entrained. The estimated entrainment rate decreases when the dry air is entrained from increasing distance from the edge of the cloud core; this is because the air farther from the edge of the cloud core is drier than the neighboring air that is within the humid shell around the cumulus cloud core. Probability density functions of entrainment rate vary with the distance and height above the cloud-base, and all are well fitted by lognormal distributions. The implications of the results for convection parameterizations are discussed. **Citation:** Lu, C., Y. Liu, S. Niu, and A. M. Vogelmann (2012), Lateral entrainment rate in shallow cumuli: Dependence on dry air sources and probability density functions, *Geophys. Res. Lett.*, *39*, L20812, doi:10.1029/2012GL053646.

1. Introduction

[2] Turbulent entrainment-mixing processes are critical to cloud-related processes such as warm rain initiation, aerosol indirect effects and cloud-climate feedbacks [*Liu et al.*, 2002]. For cumulus clouds, entrainment-mixing processes between cumulus clouds and their environment are key processes in atmospheric moist convection [e.g., *Jensen and Del Genio*, 2006].

[3] A fundamental quantity in entrainment-mixing processes is the fractional entrainment rate (λ), which is one of the strongest controls on the climate sensitivity of general circulation models (GCMs) [e.g., *Sanderson et al.*, 2008]. The tracer budget approach has been widely used to estimate λ [*Neggers et al.*, 2003], among other approaches [*Neggers et al.*, 2003; *Jensen and Del Genio*, 2006]. *Romps* [2010] introduced an approach for directly estimating λ and found that the tracer budget approach systematically underestimated λ. This conclusion was confirmed by *Dawe and Austin* [2011a]. One main reason for the difference in estimated λ lies in the origin of the entrained dry air — in the tracer budget approach, the properties of entrained air are assumed to be the mean properties of environmental air, which is equivalent to assuming that the source of dry air is distant from the edge of the cloud core. In reality, however, it is often the air from the humid shell around the cumulus that is entrained into the cloud [*Romps*, 2010; *Dawe and Austin*, 2011a]. So the distance between the edge of the cloud core and the assumed source of entrained dry air is critical to the estimation of λ. However, studies of the sensitivity of λ to the distance from edge of the cloud core are lacking. Moreover, both *Romps* [2010] and *Dawe and Austin* [2011a] drew their conclusions based on numerical simulations; thus, it is important to investigate this topic from an observational perspective. Furthermore, it has long been recognized that the entrainment process can be treated as a stochastic process and that a more realistic parameterization of convection requires the probability density function (PDF) of λ [*Romps and Kuang*, 2010]. However, observations of the PDF of λ are lacking as well.

[4] The objective of this work is to fill these two gaps by applying the recently developed mixing fraction approach [*Lu et al.*, 2012] to cumulus cloud data collected during the Routine AAF [Atmospheric Radiation Measurement (ARM) Aerial Facility] Clouds with Low Optical Water Depths (CLOWD) Optical Radiative Observations (RACORO) field campaign, which operated over the ARM Southern Great Plains (SGP) site near Lamont, Oklahoma from 22 January to 30 June 2009 [*Vogelmann et al.*, 2012]. This study investigates the PDFs of λ for different dry air sources and at different heights above cloud-base, and explores their implications for convection parameterization.

2. RACORO Data and Analysis

[5] During RACORO, the Center for Interdisciplinary Remotely-Piloted Aircraft Studies (CIRPAS) Twin Otter aircraft made comprehensive measurements of cloud, aerosol, radiation, and atmospheric state parameters. The aircraft flew at multiple levels in clouds and cloud droplet size distributions were measured by Cloud and Aerosol Spectrometer (CAS) at a 10 Hz sampling rate. The CAS probe sizes and counts aerosol particles and cloud droplets from 0.29 to 25 μm (radius) in 20 bins. Here, only the droplets with a bin-average radius larger than 1 μm are used to calculate cloud microphysical properties [e.g., droplet number concentration (N_c) and liquid water content (LWC)]. The Cloud Imaging

[1]School of Atmospheric Physics, Key Laboratory of Meteorological Disaster of Ministry of Education, Nanjing University of Information Science and Technology, Jiangsu, China.
[2]Atmospheric Sciences Division, Brookhaven National Laboratory, Upton, New York, USA.

Corresponding author: C. Lu, School of Atmospheric Physics, Key Laboratory of Meteorological Disaster of Ministry of Education, Nanjing University of Information Science and Technology, Jiangsu, China. (luchunsong110@gmail.com)

0094-8276/12/2012GL053646

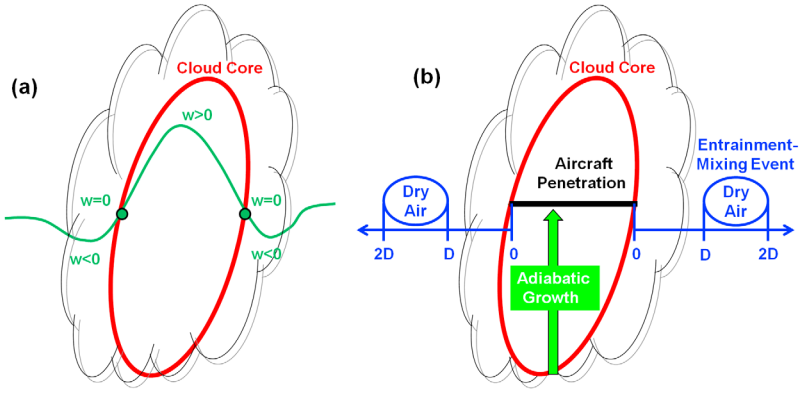

Figure 1. (a) Schematic diagram of cloud core definition. (b) Schematic diagram of the mixing fraction approach used to estimate entrainment rate. *D* can be thought of representing the size of a grid cell within a high resolution model, where its variation is studied here. See text for the details.

Probe (CIP) measured droplets in the range of 7.50 to 781 μm (radius) at 1 Hz. Temperature and water vapor were measured at 10 Hz, respectively, with a Rosemount probe and the Diode Laser Hygrometer (DLH) [*Diskin et al.*, 2002; *Podolske et al.*, 2003]. Cloud droplet size distributions with $N_c > 10$ cm^{-3} and LWC > 0.001 g m^{-3} are considered to be cloud records; using both criteria eliminates the measured size distributions that are probably composed of large aerosols instead of cloud droplets [*Zhang et al.*, 2011]. Non-drizzling clouds must further satisfy the condition that the in-cloud mean drizzle LWC (radius > 25 μm from the CIP) over the observation period was smaller than 0.005 g m^{-3}.

[6] Among 59 flights, clouds were sampled in 29 flights, and 10 flights were cumulus flights (May 22, May 23, May 24, May 26, June 11, June 15, June 19, June 23, June 24, and June 26, 2009) [*Vogelmann et al.*, 2012]. Water vapor observations were not available on May 26 or June 15, so these two flights are not included in the current analysis. To apply the mixing fraction approach to estimate λ [*Lu et al.*, 2012], individual cumulus clouds are identified in the observations from the long, horizontal flight legs. The criteria for an individual cumulus cloud are: (1) cloud droplet size distributions are considered to be within the same individual cumulus cloud when the distance between them is less than 50 m (the data were collected at ~5 m spatial resolution, based on the 10 Hz CAS sampling and an aircraft speed of ~50 m s^{-1}); (2) cloud horizontal sizes are larger than 50 m to avoid cumulus clouds that are too small for adequate sampling statistics. Because the mixing fraction approach is only applicable to growing cumulus clouds, growing cumulus clouds in the eight cases are selected using two additional criteria: (1) 80% of vertical velocity (w) in an individual cloud is positive [*Gerber et al.*, 2008; *Lu et al.*, 2012]; (2) the number of cloud droplet size distributions is larger than 30 to select relatively large cumulus clouds. Only the entrainment rate in cloud cores is estimated here. The edge of the cloud core is defined as the point along the direction from the cloud edge toward the interior of the cloud where w changes from negative to positive for the first time (Figure 1a).

3. Approach

[7] The *Lu et al.* [2012] mixing fraction approach estimates λ with smaller uncertainty than the tracer budget approach, among other advantages; using this approach, λ is calculated for each cloud penetration in this study. Instead of using the dry air properties obtained only from the aircraft's vertical sounding, we also consider dry air sources at certain distances from the edge of the cloud core. Briefly, the mixing fraction approach is schematically shown in Figure 1b. Assume that the cloud grows adiabatically from the cloud-base (z_0) to a certain level (z) where the cloud experiences lateral entrainment and isobaric mixing. The entrainment rate is calculated by,

$$\lambda = \frac{\ln \dfrac{m(z)}{m(z_0)}}{z - z_0} = \frac{-\ln \chi}{h}. \quad (1)$$

where $m(z_0)$ and $m(z)$ represent, respectively, the mass of a cloud parcel at the cloud-base and at a level z above the cloud-base, $h = z - z_0$ is the height above the cloud-base, and $\chi = m(z_0)/m(z)$ is the mixing fraction of adiabatic cloud air. The entrained mass between z_0 and z is assumed to be evenly distributed at the mid-level (h_m) above z_0:

$$h_m = (z - z_0)/2 \quad (2)$$

[8] Two properties are needed to calculate λ; the first one is h. For aircraft observations of cumuli, cloud-base height is usually determined per flight by fitting the peak LWC values at the observation levels with a linear profile [*Gerber et al.*, 2008, Figure 1; *Lu et al.*, 2012]. This approach is only applicable when cumulus clouds share a similar cloud-base during a flight; for RACORO, this approach is not applicable because cloud-base height varied during flight [*Vogelmann et al.*, 2012]. Instead, a cloud-base height is determined for each cloud as follows. The maximum LWC within a cumulus cloud is assumed to be the adiabatic LWC. The cloud-base height and thus h are estimated by assuming adiabatic growth. Note that the assumed adiabatic LWC along a leg might be less than the true adiabatic LWC because of potential influence of entrainment-mixing processes. Nevertheless, the effect on the estimated λ is likely small because of the cancellation of effects on h and χ in Eq. (1): when the true adiabatic LWC is used in the calculation, h increases because it needs a larger height to obtain the true adiabatic LWC; -lnχ increases because χ generally has a concurrent variation with the ratio of LWC to its adiabatic value and χ decreases. If we

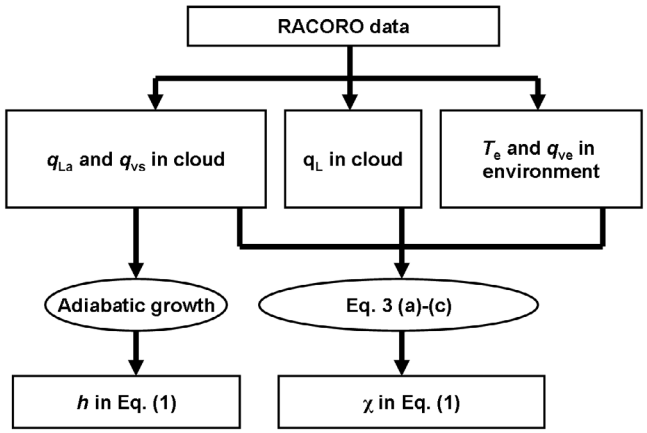

Figure 2. Flow chart for the calculation of height (h) and the mixing fraction of adiabatic cloud air (χ) in Equation (1). See text for the meanings of the symbols.

assume that the maximum LWC is 0.8 of the true adiabatic LWC, the computed relative difference between the entrainment rate with the assumed adiabatic LWC and that with the true adiabatic LWC is 10% to 16% for different D (D will be explained later).

[9] The second property is χ; it is calculated based on the conservation of total water and energy during the mixing at z. The conservation equations were represented by Eq. (5) in the study by *Lu et al.* [2012] as:

$$q_L + q_{vs}(T) = \chi[q_{vs}(T_a) + q_{La}] + (1-\chi)q_{ve} \tag{3a}$$

$$c_p T = c_p T_a \chi + c_p T_e (1-\chi) - L_v(q_{La}\chi - q_L) \tag{3b}$$

$$q_{vs}(T) = 0.622 \frac{e_s(T)}{p - e_s(T)} \tag{3c}$$

where: T, $q_{vs}(T)$ and q_L are, respectively, the mean temperature, saturation vapor mixing ratio and liquid water mixing ratio in cloud cores; T_e and q_{ve} are, respectively, the temperature and water vapor mixing ratio of the entrained dry air; T_a, $q_{vs}(T_a)$ and q_{La} are, respectively, the temperature, saturation vapor mixing ratio, and liquid water mixing ratio in the adiabatic cloud parcel; and e_s, p, c_p, and L_v are, respectively, the saturation vapor pressure at T, air pressure, specific heat capacity at constant pressure and latent heat. As shown in Figure 2, the input parameters for this simple model are q_{La}, $q_{vs}(T_a)$, q_L, T_e, and q_{ve}. In-cloud temperature observations are only used to calculate air density in order to convert LWC to liquid water mixing ratio.

[10] As illustrated in Figure 1b, the environment's temperature and water vapor mixing ratio are the mean values from the air that is D to $2D$ from the edge of the cloud core on both sides of the aircraft's cloud penetration. D can be thought of representing the size of a grid cell within a high resolution model. Sometimes, cloud cores are too close and the entrained air for one core (from D to $2D$) would be affected by a neighboring core. This would be the case, for example, if the aircraft is flying (right to left) from one core, C1, towards another, C2, and distance between their core edges is less than $3D$. In this case, the leftward dry air for C1 is abandoned, and only the rightward dry air for C1 is used; if the rightward dry air is also too close to another cloud core, similar to the leftward dry air, then this cloud is not counted. One hundred eighty six cumulus clouds satisfy all the conditions and are analyzed here.

4. Results

4.1. Distance Dependence

[11] To examine the dependence of λ on D, we estimate λ over a range of D, i.e., 10 m, 20 m, 30 m, 40 m, 50 m, 100 m, 300 m, and 500 m. Figure 3a shows that the mean λ significantly decreases from 2.8 to 1.4 km^{-1} as D increases from 10 m to 100 m; λ is less sensitive to D variation from 100 m to 500 m. Note that λ of 2.8 km^{-1} for D = 10 m is well within the range of λ ($\sim$1.8 to $\sim$5.1 km^{-1}) obtained directly from a cloud-resolving simulation by *Romps* [2010]. The green dot and bar in Figure 3a are the mean of λ and standard error of the mean when the temperature and relative humidity of the entrained dry air are obtained from the aircraft vertical sounding at the same height as the horizontal leg. This dry air is far from cloud cores ($D \gg 500$ m), but the results are close to those for D = 500 m. Thus the dry air within D to $2D$ (with D varies between 10 and 500 m) most likely represents all possible dry air sources in the lateral mixing processes. Note that when the dry air properties are taken from the sounding, the estimated entrainment rate is similar to that obtained using the tracer budget approach [*Lu et al.*, 2012].

[12] The decrease of λ with increasing D is consistent with the numerical results by *Romps* [2010] and *Dawe and Austin* [2011a], in which their analysis of model simulations found that the tracer budget approach underestimated λ. In the tracer budget approach, the temperature and relative humidity of the dry air are assumed to be averages of the non-cloud environment; such dry air properties are expected to be close to the properties from the sounding or when D = 500 m in this study. Using their simulations, *Dawe and Austin* [2011a] diagnosed that it was the moistest parts of the shell around cumulus clouds that were entrained into cloud cores; so the dry air properties are expected to be close to the properties when D = 10 m. Thus our observational results confirm the simulation-based conclusions in *Romps* [2010] and *Dawe and Austin* [2011a].

[13] As mentioned above, the presence of a downdraft shell that surrounds the cloud accounts for the difference between the λ determined from the tracer budget approach and directly obtained from simulated fields [*Romps*, 2010; *Dawe and Austin*, 2011a]. To further examine the effects of the shells, Figures 3b and 3c show the relative humidity and temperature in the dry air as a function of D. Similar to λ, relative humidity decreases significantly as D increases from 10 to 100 m, and decreases slightly more as D increases from 100 to 500 m. In contrast, temperature generally increases slowly with increasing D. The higher relative humidity and lower temperature for smaller D is due to evaporative cooling in the shells around the cloud cores. Similar phenomena have been found in other studies [e.g., *Heus and Jonker*, 2008].

[14] The above calculation of λ is based on three arbitrary thresholds given in Section 2 that are used to select cumulus clouds; the sensitivity of λ to them is tested next. The first arbitrary threshold is "50 m"; when the distance between two cloud droplet size distributions is less than 50 m, the two

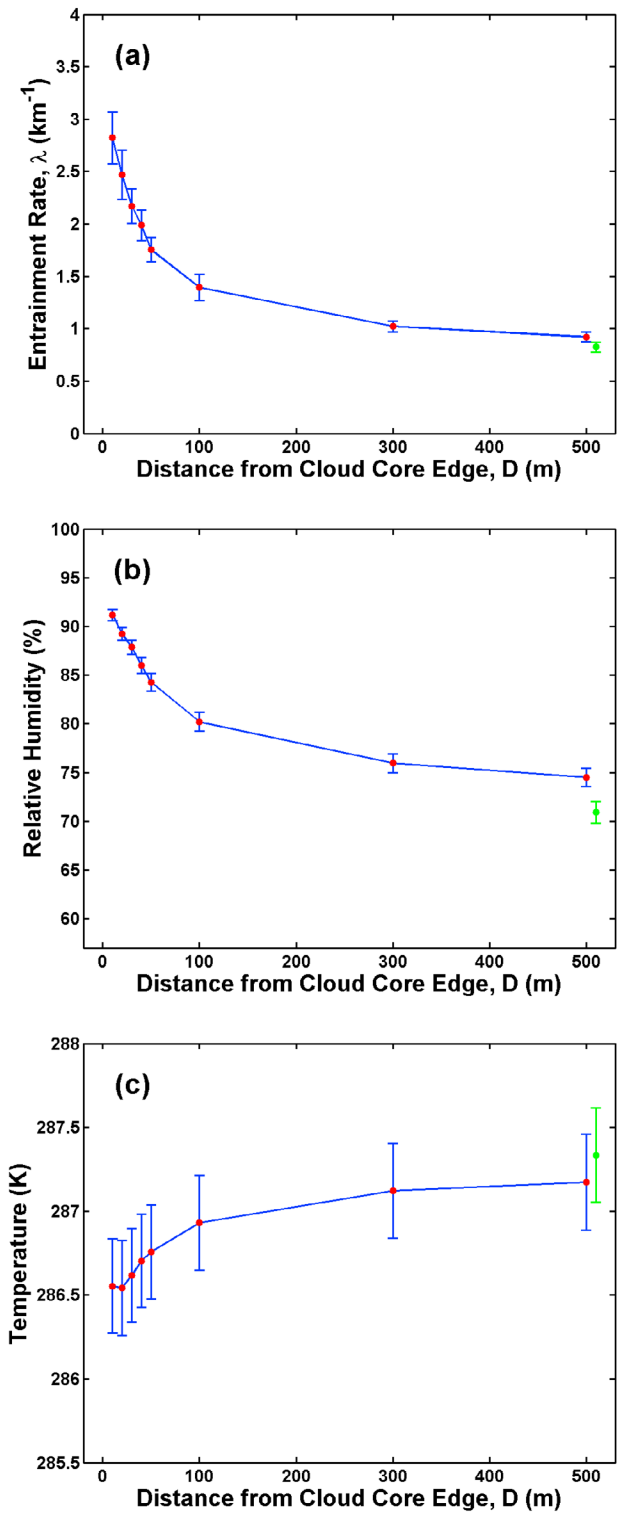

Figure 3. (a) Entrainment rate (λ), (b) relative humidity and (c) temperature as a function of D for eight cumulus flights. The dry air is assumed to be from D to $2D$ away from the edge of the cloud core (see Figure 1 and text for the details). The bars represent standard error of the mean of the ordinate property. The green dots and bars, respectively, show the corresponding mean and standard error of the mean when the dry air properties are obtained from aircraft vertical soundings at the cloud penetration level, where the x-axis values of the green dots are arbitrary.

distributions are considered to be in the same cumulus cloud. Taking the λ calculated using 50 m as a reference, the λ using 25 m and 75 m have relative differences of 3% to 6% for different D. The second one is "30", which is the minimum number of cloud droplet size distributions required for the cloud to be sufficiently large. Taking the λ calculated using 30 as a reference, the λ using 15 and 45 have relative differences of 4% to 8% for different D. The third one is "0 m s^{-1}", which is the vertical velocity used to define the cloud cores. Taking the λ calculated using 0 m s^{-1} as a reference, the λ using 0.5 m s^{-1} has relative differences of 5% to 7% for different D.

4.2. PDF of λ

[15] The standard deviation of λ is equal to the product of the standard error of the mean as shown in Figure 3a and square root of the cumulus number, 186; thus the standard deviation is expected to be large, suggesting that the mean value alone is not enough to describe the variation of λ and calls for knowledge of the PDF of λ. *Romps and Kuang* [2010] found that assuming a random λ in a stochastic parcel model, instead of a constant λ, could reproduce the total cloud-updraft mass flux and other related properties obtained from large eddy simulations. Figure 4 shows the PDFs of λ in cumulus clouds for different D and the PDF of λ when the properties of dry air are taken from soundings. All the PDFs can be well fitted by lognormal distributions, with coefficients of determination (R^2) $\geq$ 0.96.

[16] The penetration levels in different cumulus clouds had different heights above cloud-base, so combining these data enables an examination of the vertical profiles of entrainment rate and their PDFs. Figure S1 in auxiliary material Text S1 shows the vertical profiles of λ for D = 10 m, 50 m and 500 m, whose profiles are representative of the other values of D (See the auxiliary material for the details); λ decreases with the increasing height, as expected from Equation (1), which is consistent with some previous results [*Neggers et al.*, 2003; *Gerber et al.*, 2008; *Dawe and Austin*, 2011b; *Lu et al.*, 2012] but contrary to others [*Romps*, 2010].[1] The PDFs of λ at different levels also follow lognormal distributions with $R^2 \geq 0.95$ (See the auxiliary material for the details). It is noteworthy that λ along the lower legs decrease more significantly with increasing D than that along the higher legs (Figure S1 in Text S1; see the auxiliary material for the details). The reason is that, for the lower legs, h in Equation (1) is smaller and $1/h$ is larger; thus, λ is more sensitive to the variation of $-\ln\chi$ caused by the increasing D. As a result, the λ along the lower legs have larger contributions to the distance dependence of entrainment rate as shown in Figure 3a.

5. Important Implications for Convection Parameterization

[17] The wide variability of λ suggests that these clouds were affected by entrainment-mixing processes to different extents within the domain of aircraft observations, where the lengths of the horizontal flight legs were ~30 km. This is supported by the positive correlation between λ and the spatial relative dispersion of LWC (i.e., the ratio of standard deviation of LWC to mean LWC), as shown in the auxiliary

[1]Auxiliary materials are available in the HTML. doi:10.1029/2012GL053646.

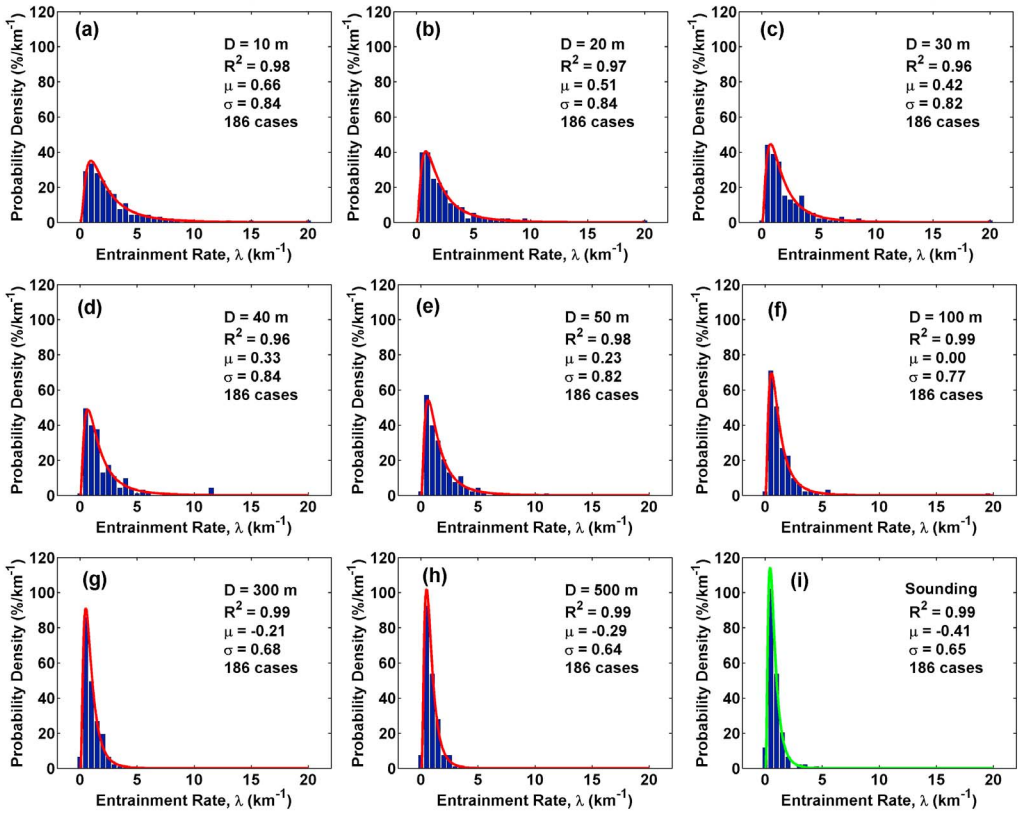

Figure 4. Probability density functions (PDFs) of entrainment rate (λ) for different dry air sources in eight cumulus flights. (a–h) The dry air is assumed to be from D to $2D$ away from the edge of the cloud core (see Figure 1 and text for the details); (i) the dry air properties are assumed from aircraft vertical sounding at the cloud penetration level. The λ bin width for the PDFs is 0.5 km^{-1}. Each panel provides the coefficient of determination (R^2), and the mean (μ) and standard deviation (σ) of $\ln(\lambda)$ and a plot of the lognormal fit.

material. The typical grid size of current climate models is ~100 km; thus, it is expected that the unresolved cumulus clouds across a GCM grid cell are affected by entrainment-mixing processes to varying degrees. Taking these cumulus clouds as parcels or plumes, multiple-parcel models [*Neggers et al.*, 2002] and multiple mass-flux parameterizations [*Sušelj et al.*, 2012] also emphasize the importance of representing the variation of λ.

[18] The dependence of λ on D poses a question as to what the appropriate D is for λ (or PDF of λ) that should be used in numerical models. For the two-layer entraining plume parameterizations, where only cloud and cloud-free environmental air are considered, *Dawe and Austin* [2011a] argue that the entrainment rate from the tracer budget approach is best; thus it is recommended to use the PDF of λ for larger D (e.g., 300 m or 500 m). In the three-layer model proposed by *Heus and Jonker* [2008], the shell around cumulus clouds is considered in addition to the cloud and environmental air. In this case, the shell plays a critical role in the lateral mixing between cloud and environment; thus, the entrainment rate at smaller D (e.g., 10 m or 20 m) is recommended. The model resolution is clearly also a factor of concern, where a smaller D should be associated with a finer grid spacing.

6. Concluding Remarks

[19] Using a mixing fraction approach recently developed by *Lu et al.* [2012], entrainment rates are estimated in cloud cores for 186 non-drizzling, growing cumulus clouds observed during RACORO, where we focus on dependence of entrainment rate on the distance from the cloud core from which the dry air is entrained and the resulting probability distributions. The results show that, due to the presence of humid shells around the cumulus clouds, the mean λ decreases with the increasing distance from the edge of the cloud core, which is consistent with the conclusions by *Romps* [2010] and *Dawe and Austin* [2011a] that are based on numerical simulations. All of the PDFs of λ can be well fitted by lognormal distributions (all $R^2 \geq 0.96$), regardless of the dry air source or the height above cloud-base.

[20] The reason for the wide spread λ (and their resulting PDFs) is that different clouds are affected by entrainment-mixing processes to differing degrees. The PDF of λ has a potential application in improving convection parameterizations in large scale models. Due to the dependence of λ on D, the PDF of λ for larger D is recommended for two-layer (cloud and environment) entraining plume parameterizations, whereas that for smaller D is recommended for three-layer (cloud, environment and shell between them) parameterizations.

[21] To the authors' knowledge, this work provides the first observational studies of the distance dependence of λ and its PDFs for shallow cumulus clouds. Much remains to be learned. First, this study focuses on continental cumuli and studies are needed on maritime cumuli. Second, as discussed by *Lu et al.* [2012], aliasing problems in aircraft observations may affect the result. It is well known that

entrainment events are likely driven by turbulent eddies ranging from the Kolmogorov microscopic scale to the macroscopic cloud size [*Gerber et al.*, 2008]; however, most aircraft measurements cannot resolve the detailed effects of eddies smaller than the sampling resolution (e.g., ∼5 m in this study). Analysis of higher-resolution observations warrants further study. Numerical models with different resolutions are also a good choice to explore scale effects [*Guo et al.*, 2008]. Another issue in aircraft observations can be hysteresis effects in the measurements. The DLH used here for measurements of the water vapor mixing ratio is based on an optical measurement of the strength of a water vapor line [*Diskin et al.*, 2002], which does not have the hysteresis effect [*Glenn Diskin*, Personal Communication]. Temperature measured by Rosemount might have this effect; however, as shown in Figure 3c, temperature is lower for smaller D due to evaporative cooling in the shells around the cloud cores, consistent with other studies [e.g., *Heus and Jonker*, 2008] and, thus, the temperature observations here seem to be reasonable around cumulus clouds. Third, entrainment rate and entrainment-mixing mechanisms [e.g., *Lu et al.*, 2011] are expected to be closely related with one another. How to investigate the relationship between them warrants further investigation.

[22] **Acknowledgments.** Lu, Liu and Vogelmann were supported by the U.S. Department of Energy's (DOE) Earth System Modeling (ESM) program via the FASTER project (www.bnl.gov/esm) and Atmospheric System Research (ASR) program (DE-AC02-98CH10886). Niu was supported by the Qing-Lan Project for Cloud-Fog-Precipitation-Aerosol Study in Jiangsu Province, China, a Project Funded by the Priority Academic Program Development of Jiangsu Higher Education Institutions. Data used in this article are from the U.S. Department of Energy ARM Aerial Facility's RACORO Campaign. We appreciate the helpful discussions about the CAS with Haf Jonsson, Greg McFarquhar and Hee-Jung Yang. We also appreciate Glenn Diskin's help on the data from DLH.

[23] The editor thanks two anonymous reviewers for assistance evaluating this manuscript.

References

Dawe, J. T., and P. H. Austin (2011a), The influence of the cloud shell on tracer budget measurements of LES cloud entrainment, *J. Atmos. Sci.*, *68*(12), 2909–2920, doi:10.1175/2011JAS3658.1.

Dawe, J. T., and P. H. Austin (2011b), Interpolation of LES cloud surfaces for use in direct calculations of entrainment and detrainment, *Mon. Weather Rev.*, *139*(2), 444–456, doi:10.1175/2010MWR3473.1.

Diskin, G. S., J. R. Podolske, G. W. Sachse, and T. A. Slate (2002), Open-path airborne tunable diode laser hygrometer, *Proc. SPIE Int. Soc. Opt. Eng.*, *4817*, 196–204, doi:10.1117/12.453736.

Gerber, H. E., G. M. Frick, J. B. Jensen, and J. G. Hudson (2008), Entrainment, mixing, and microphysics in trade-wind cumulus, *J. Meteorol. Soc. Jpn.*, *86A*, 87–106, doi:10.2151/jmsj.86A.87.

Guo, H., Y. Liu, P. H. Daum, X. Zeng, X. Li, and W. K. Tao (2008), Effects of model resolution on entrainment (inversion heights), cloud-radiation interactions, and cloud radiative forcing, *Atmos. Chem. Phys. Discuss.*, *8*(6), 20,399–20,425, doi:10.5194/acpd-8-20399-2008.

Heus, T., and H. J. J. Jonker (2008), Subsiding shells around shallow cumulus clouds, *J. Atmos. Sci.*, *65*(3), 1003–1018, doi:10.1175/2007JAS2322.1.

Jensen, M. P., and A. D. Del Genio (2006), Factors limiting convective cloud-top height at the ARM Nauru Island Climate Research Facility, *J. Clim.*, *19*(10), 2105–2117, doi:10.1175/JCLI3722.1.

Liu, Y., P. H. Daum, S. K. Chai, and F. Liu (2002), Cloud parameterizations, cloud physics, and their connections: An overview, *Recent Res. Dev. Geophys.*, *4*, 119–142.

Lu, C., Y. Liu, and S. Niu (2011), Examination of turbulent entrainment-mixing mechanisms using a combined approach, *J. Geophys. Res.*, *116*, D20207, doi:10.1029/2011JD015944.

Lu, C., Y. Liu, S. S. Yum, S. Niu, and S. Endo (2012), A new approach for estimating entrainment rate in cumulus clouds, *Geophys. Res. Lett.*, *39*, L04802, doi:10.1029/2011GL050546.

Neggers, R. A. J., A. P. Siebesma, and H. J. J. Jonker (2002), A multiparcel model for shallow cumulus convection, *J. Atmos. Sci.*, *59*(10), 1655–1668, doi:10.1175/1520-0469(2002)059<1655:AMMFSC>2.0.CO;2.

Neggers, R. A. J., P. G. Duynkerke, and S. M. A. Rodts (2003), Shallow cumulus convection: A validation of large-eddy simulation against aircraft and Landsat observations, *Q. J. R. Meteorol. Soc.*, *129*(593), 2671–2696, doi:10.1256/qj.02.93.

Podolske, J. R., G. W. Sachse, and G. S. Diskin (2003), Calibration and data retrieval algorithms for the NASA Langley/Ames Diode Laser Hygrometer for the NASA Transport and Chemical Evolution Over the Pacific (TRACE-P) mission, *J. Geophys. Res.*, *108*(D20), 8792, doi:10.1029/2002JD003156.

Romps, D. M. (2010), A direct measure of entrainment, *J. Atmos. Sci.*, *67*(6), 1908–1927, doi:10.1175/2010JAS3371.1.

Romps, D. M., and Z. Kuang (2010), Nature versus nurture in shallow convection, *J. Atmos. Sci.*, *67*(5), 1655–1666, doi:10.1175/2009JAS3307.1.

Sanderson, B., C. Piani, W. J. Ingram, D. A. Stone, and M. R. Allen (2008), Towards constraining climate sensitivity by linear analysis of feedback patterns in thousands of perturbed-physics GCM simulations, *Clim. Dyn.*, *30*(2–3), 175–190, doi:10.1007/s00382-007-0280-7.

Sušelj, K., J. Teixeira, and G. Matheou (2012), Eddy diffusivity/mass flux and shallow cumulus boundary layer: An updraft PDF multiple mass flux scheme, *J. Atmos. Sci.*, *69*(5), 1513–1533, doi:10.1175/JAS-D-11-090.1.

Vogelmann, A. M., et al. (2012), RACORO extended-term aircraft observations of boundary layer clouds, *Bull. Am. Meteorol. Soc.*, *93*(6), 861–878, doi:10.1175/BAMS-D-11-00189.1.

Zhang, Q., J. Quan, X. Tie, M. Huang, and X. Ma (2011), Impact of aerosol particles on cloud formation: Aircraft measurements in China, *Atmos. Environ.*, *45*, 665–672, doi:10.1016/j.atmosenv.2010.10.025.